Appl Phys B (2011) 105:675–679
DOI 10.1007/s00340-011-4809-4

Applied Physics B
Lasers and Optics

RAPID COMMUNICATION

Single 10-fs deep-ultraviolet pulses generated by broadband four-wave mixing and high-order dispersion compensation

Y. Kida · J. Liu · T. Kobayashi

Received: 7 June 2011 / Revised version: 25 September 2011 / Published online: 17 November 2011

Abstract Broadband chirped-pulse four-wave mixing and a pulse compressor consisting of a prism pair and a grating pair are used to generate 10.3-fs deep-ultraviolet pulses. A large proportion of the dispersion up to 1000 fs^2 is compensated without inducing third-order dispersion, which together with the smooth spectral and temporal profiles of the pulses makes them suitable for ultrafast spectroscopy. Unexpected spectral narrowing is observed when short input pulses were used for four-wave mixing. This narrowing is explained in terms of other third-order nonlinear phenomena, namely self-phase and cross-phase modulations, which occur simultaneously with four-wave mixing.

1 Introduction

Real-time vibrational spectroscopy using pulses shorter than molecular vibration periods has been extensively used to study relaxation of electronically excited states and vibrational dynamics of molecules [1, 2]. Simultaneous measurements have made it possible to study the molecular structural changes that occur during chemical relaxations [3–5]. Such experiments have been performed using ∼5-fs visible pulses from a noncollinear optical parametric amplifier. Ultrashort (∼10 fs) deep-ultraviolet (DUV) pulses are anticipated to be useful for investigating DUV photochemistry in biologically important molecules that absorb DUV such as DNA and proteins, which cannot be excited by visible pulses. However, sub-10-fs DUV pulses have not yet been applied to spectroscopy despite 10-fs and shorter DUV laser pulses having been generated by several approaches [6–10]. The main difficulty in applying short DUV pulses is the large group-delay dispersion (GDD) generated even in transparent media such as air and the sample cell windows used in pump–probe spectroscopy. This problem is more acute in the DUV region than in the near UV and visible regions. This GDD needs to be compensated for without inducing third-order dispersion (TOD), otherwise satellite pulses will be generated in the temporal profile.

Several approaches have been used to simultaneously compensate for GDD and TOD, including methods based on using a prism and grating compressors [11, 12], a deformable mirror [13–15], and an acousto-optic programmable dispersive filter [16, 17]. Of these methods, the pulse compressor consisting of prism and grating pairs has superior cost effectiveness and it has been utilized to generate few-cycle pulses [11, 12]. A broadband DUV light source is required for generating 10-fs and shorter DUV pulses. A technique based on broadband chirped-pulse four-wave mixing (BCP-FWM) has been proposed for this objective [18]. BCP-FWM can compensate positive group-velocity dispersion in transparent media; however, to compensate for positive GDD as large as 1000 fs^2, the pulse en-

Y. Kida (✉) · J. Liu · T. Kobayashi
Advanced Ultrafast Laser Research Center, University of Electro-Communications, 1-5-1 Chofugaoka, Chofu, Tokyo 182-8585, Japan
e-mail: kida@ils.uec.ac.jp
Fax: +81-42-4435825

Y. Kida · J. Liu · T. Kobayashi
JST, CREST, 5 Sanbancho, Chiyoda-ku, Tokyo 102-0075, Japan

T. Kobayashi
Department of Electrophysics, National Chiao-Tung University, 1001 Ta Hsueh Rd., Hsinchu 300, Taiwan

T. Kobayashi
Institute of Laser Engineering, Osaka University, 2-6 Yamada-oka, Suita, Osaka 565-0971, Japan

ergy of the DUV pulse generated by BCP-FWM becomes very low.

This communication reports the generation of 10-fs DUV pulses by compensating a GDD of about 1000 fs^2. The laser system used is based on BCP-FWM and a pulse compressor consisting of a prism pair and a grating pair. This system is capable of producing both a smooth broadband spectrum and single pulses. By using short input pulses for BCP-FWM, a conversion efficiency into DUV pulses was obtained that was nine times greater than that obtained in a previous study [18]. As a result, a DUV pulse that was suitable for ultrafast spectroscopy was generated with a pulse energy of 150 nJ (even after lossy pulse compressors). Depending on the spectral width of the input idler pulse, narrowband DUV pulses were generated despite the use of a broadband input idler pulse. The origin of this undesirable phenomenon is explained in terms of the frequency chirps of the input pulses and energy conservation in the four-wave mixing (FWM) process.

2 Experimental

Similar to a previous study [18], a near-infrared (NIR) pulse with a pulse duration of 35 fs, a repetition rate of 1 kHz, and a center wavelength of 800 nm was generated by a Ti:sapphire chirped-pulse amplifier. A portion of the pulse energy was used to generate a broadband NIR pulse (idler pulse) through self-phase modulation (SPM) in a hollow fiber (length: 600 mm; core diameter: 250 µm; 0.5-mm-thick fused-silica windows) filled with Kr gas (0.80 atm). The remainder of the pulse energy was converted into a second-harmonic near-ultraviolet (NUV; wavelength: 400 nm) pulse in a 0.2-mm-thick β-BaB_2O_4 crystal. The broadband NIR pulse was reflected six times off chirped mirrors (Layertec) with a negative GDD of -40 fs^2, whereas the NUV pulse (pump pulse) was compressed to a nearly transform-limited pulse by a prism pair. The positive frequency chirp in the NIR pulse was not completely compensated for and the NIR pulse was broader than the pump pulse. After being combined collinearly by a 0.5-mm-thick dichroic mirror (fused silica substrate, Laser Components GmbH), the idler and pump pulses were focused into a hollow fiber (second hollow fiber; length: 550 mm; core diameter: 140 µm; 0.5-mm-thick MgF_2 windows) filled with Ar gas (0.09 atm) using an aluminum-coated concave mirror with a focal length of 750 mm. The second hollow fiber was 550 mm long and had a core diameter of 140 µm. The pump and idler, respectively, had pulse energies of 90 and 60 µJ in front of the second hollow fiber chamber. After collimation by another concave mirror with a focal length of 750 mm, the generated p-polarized DUV pulse passed through a grating compressor and a prism compressor. These compressors consisted of two gratings (blaze wavelength: 240 nm; groove density: 240 lines/mm; incidence angle: 5°) and two calcium fluoride prisms with low-dispersion dielectric mirrors (for s-polarization, Lattice Electro Optics). The apex separation between the two prisms was 89 mm and the separation between the two gratings was 535 mm. This introduces a GDD and TOD of -950 fs^2 and -460 fs^3 at 267 nm, respectively. This amount of GDD is difficult to be obtained by the use of only one of the compressors without substantial satellite-pulse generation. The DUV pulse emerging from the compressor was characterized using a dispersion-free self-diffraction frequency-resolved optical-gating (FROG) [19] that used a 100-µm-thick sapphire plate as the nonlinear medium.

3 Results and discussion

The two input beams into the second hollow fiber were carefully aligned collinearly, and the coupling of the beams was optimized by maximizing the output signal energy. The center wavelength of the signal depended on the time delay between the idler and pump pulses because of the positive chirp of the input idler. The delay was adjusted to lead to maximum temporal overlap between the two input pulses, i.e., the pump pulse was overlapped with the center part of the idler. The center wavelength of the signal depends sensitively on the time delay when the chirp rate of the idler is large.

The DUV pulse from the hollow fiber had a pulse energy of 2 µJ, which decreased to 150 nJ after the pulse had passed through the pulse compressors and been reflected from several aluminum mirrors that guide the pulse into the autocorrelator. The use of the aluminum mirrors was because a broadband low dispersion mirror was not available for p-polarization and for a small angle of incidence. The grating compressor and prism compressor, respectively, had energy throughputs of 24% and 96%, giving a total energy throughput of 17%. The resultant pulse energy of 150 nJ is sufficient for pump-probe spectroscopy. The energy may be improved by replacing the grating pair by broadband chirped mirrors when it will be available in the future. In addition, since the energy conversion efficiency depends nonlinearly on the intensity of the pump pulse, increase in the pump pulse energy results in substantial increase in the signal pulse energy [20]. As Fig. 1(a) shows, the generated DUV pulse has a smooth spectrum despite the spectrum of the input idler pulse containing sharp structures [Fig. 1(b)]. This is because the input idler pulse is slightly longer than the input pump pulse, as discussed in [20].

Figure 2(a) shows the measured self-diffraction-FROG trace for the compressed DUV pulse. The trace was analyzed using commercial software (FROG 3.0, Femtosoft Technologies). Figure 2(b) shows the retrieved trace from the

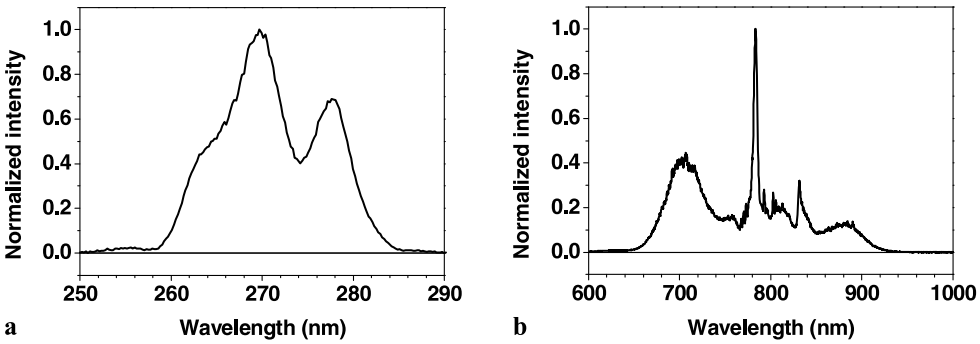

Fig. 1 Spectra of (**a**) the output DUV pulse and (**b**) the idler pulse

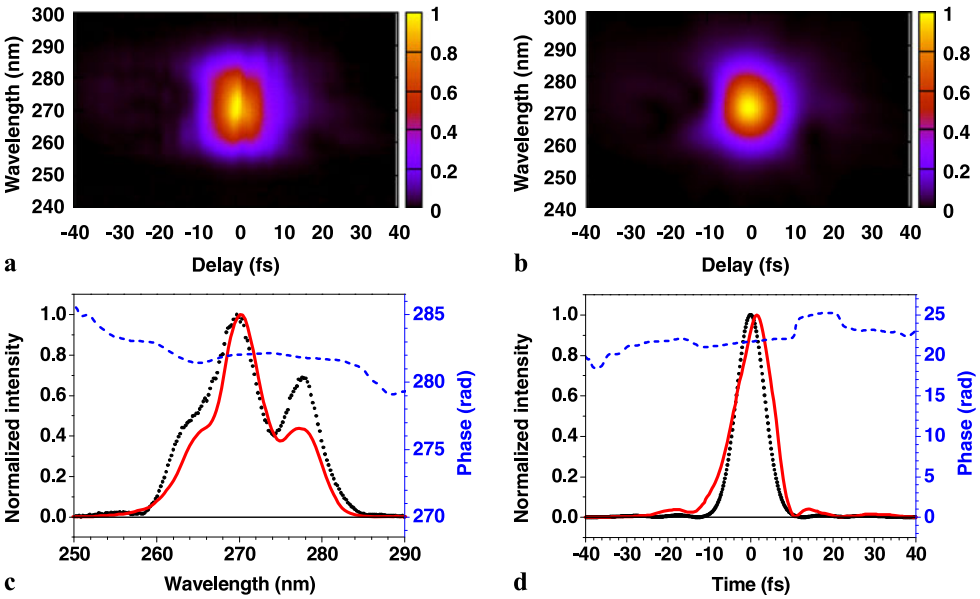

Fig. 2 (**a**) Measured and (**b**) retrieved FROG traces. (**c**) The spectrum measured with the spectrometer (*dotted line*), the spectrum (*solid line*), and the spectral phase (*broken line*) retrieved from the FROG traces are shown. (**d**) The temporal intensity profile of the transform-limited pulse corresponding to the measured spectrum is shown by the *dotted line*, and the retrieved temporal intensity profile and phase are indicated by the *solid* and *broken lines*, respectively

analysis; the FROG error in the retrieval was 0.007, which indicates a high retrieval accuracy. Figure 2(c) depicts the retrieved spectrum; it shows good agreement with the spectrum measured using a spectrometer [dotted line in Fig. 2(c); it is the same as Fig. 1(a)]. The retrieved spectral phase is not substantially distorted by GDD or TOD with a small variation of 0.8 rad over the range 262 to 283 nm. The peak intensity of the pedestal component of the retrieved temporal profile is 25 times lower than that of the main pulse. The temporal profile consists of nearly a single pulse with a duration of 10.3 fs. The transform-limited pulse duration of the pulse is 8.0 fs, which was calculated using the measured spectrum shown in Fig. 1(a). The 29% difference in the pulse durations may be due to residual high-order dispersion that could not be compensated by the compressors. However, it is expected that this 10-fs DUV pulse can easily be used for ultrafast pump−probe spectroscopy. In DUV ultrafast spectroscopy of a sample in solution, it is preferable not to use a fused-silica cell because two-photon absorption may occur. Instead, it is better to use a cell with CaF_2 windows. Since the prism compressor used to compress the DUV pulse contains prisms made of CaF_2, the group-velocity dispersion in the sample cell can be easily and precisely precompensated by simply varying the insertion of the second prism of the prism-pair compressor.

Using a broader input pulse spectrum might be expected to generate a signal DUV pulse with a broader spectrum in the BCP-FWM process. However, the opposite observation was made in the present experiment. The output DUV pulse spectrum from the second hollow fiber chamber depended on the Kr pressure in the first hollow fiber, as shown in Fig. 3(a). When the Kr pressure was $<10^{-4}$ atm and the NIR pulse was not spectrally broadened in the first hollow fiber, the DUV pulse generated by the FWM had a full width at half maximum (FWHM) of 8 nm. Even though the input idler pulse bandwidth increased monotonically in the first hollow fiber when the gas pressure was increased from 0 to 0.78 atm, the spectral width of the DUV pulse decreased with increasing gas pressure until the FWHM reached a minimum of 4 nm (between 0.27 and 0.4 atm), as shown in Fig. 3(b). At Kr pressures above 0.4 atm, the DUV pulse bandwidth increased with increasing gas pressure.

This behavior can be explained by energy conservation in FWM. Energy conservation in the FWM process can

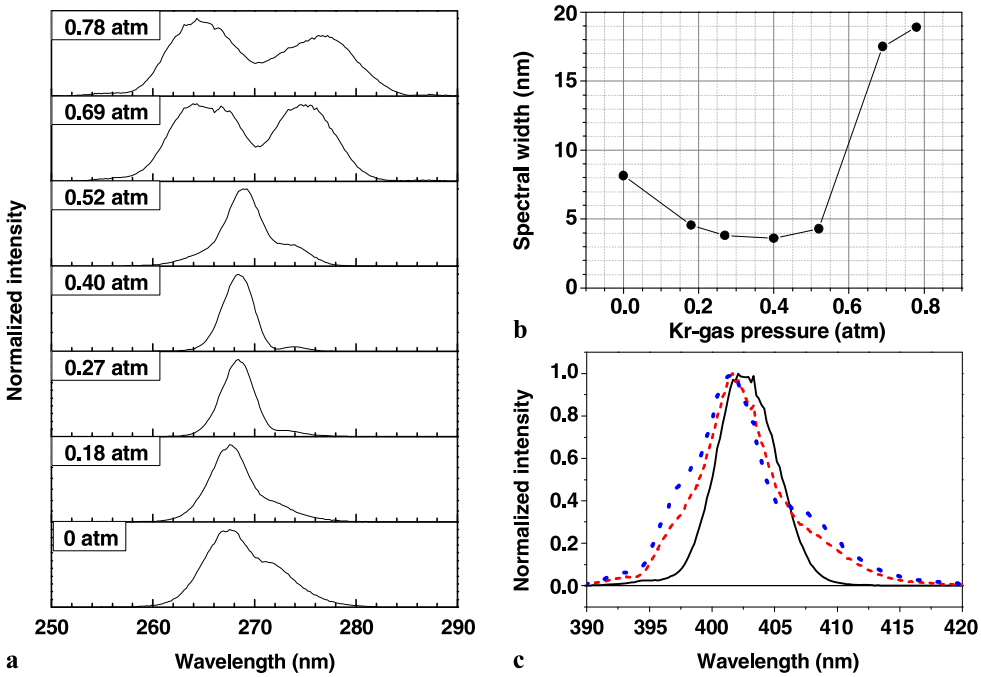

Fig. 3 (**a**) Dependence of spectra and (**b**) FWHM of the DUV pulses from the hollow fiber on the pressure of Kr-gas in the first hollow fiber. (**c**) Spectra of the input (*solid line*) and output pump pulses from the hollow fiber. *Dotted line* corresponds to the spectrum of the output pump pulse measured when both the pump and idler pulses were coupled to the hollow fiber, whereas *broken line* was obtained when only the pump pulse was coupled

be expressed by $\omega_{\text{pump}} + \omega_{\text{pump}} - \omega_{\text{idler}} = \omega_{\text{signal}}$, where ω_{pump}, ω_{idler}, and ω_{signal} are the pump, idler, and signal angular frequencies, respectively. When the pump and idler pulses are linearly chirped, the angular frequencies of the pump and idler pulses are $\omega_{\text{pump}}(t) = 2\omega_0 + \beta_{\text{pump}}t$ and $\omega_{\text{idler}}(t) = \omega_0 + \beta_{\text{idler}}t$, respectively. Here, ω_0 is the center angular frequency of the idler and β_{pump} and β_{idler} are the chirp rates of the pump and idler pulses, respectively. Energy conservation gives the DUV signal pulse frequency, $\omega_{\text{signal}}(t) = 3\omega_0 + (2\beta_{\text{pump}} - \beta_{\text{idler}})t$. The frequency chirps of the idler and pump pulses cancel each other out when the frequency chirps of the two input pulses have the same signs. When $2\beta_{\text{pump}} - \beta_{\text{idler}} = 0$ is satisfied, no frequency chirp is induced in the signal pulse. Since the pump pulse is shorter than the idler pulse, the duration of the temporal overlap between the two input pulses, and thus the signal-pulse width, are mainly determined by the pump-pulse duration. By the increase in the gas-pressure in the first hollow fiber, the chirp rate of the signal changes according to the increase in the chirp rate of the idler while the signal pulse duration does not change appreciably. For a given temporal profile of a pulse, the smaller the chirp rate, the narrower the bandwidth of a pulse [21]. The narrowest bandwidth is therefore obtained at a certain gas-pressure at which no frequency chirp is introduced in the signal pulse.

In the present experiment, frequency chirps were induced in the input pulses by SPM in the first hollow fiber as well as by the prism pair and the windows of the hollow-fiber chambers. The peak intensity of the input NUV pump pulse was sufficiently high to induce SPM in the second hollow fiber and SPM induced a positive chirp in the pump pulse during propagation, as was also observed in a previous study [6]. Cross-phase modulation due to the interaction between the pump and idler also slightly broadened the spectral width of the pump pulse. When only the pump pulse was coupled to the hollow fiber, the pump pulse spectrum was broadened and the output pump pulse spectrum extended from 390 to 417 nm. On the other hand, the input pulse spectrum extended from 390 to 410 nm, which is slightly narrower than the output spectrum of the pump pulse. The pump pulse spectrum changed when the idler and pump pulses were simultaneously coupled to the fiber [Fig. 3(c)], although the spectral range was similar to that obtained when the idler pulse was not coupled. The input idler pulse was also positively chirped. The frequency chirp was induced by the SPM in the first hollow fiber and was not completely compensated by the chirped mirrors. The chirp rate of the input idler pulse depended on the SPM efficiency and hence on the Kr pressure. The pump and idler pulses were thus positively chirped during the FWM interaction. When the Kr pressure was lower than 0.27 atm, two times the chirp rate of the pump pulse, $2\beta_{\text{pump}}$, was greater than that of the idler β_{idler}. For Kr pressures between 0.27 and 0.40 atm, $2\beta_{\text{pump}}$ was nearly equal to β_{idler} and the minimum spectral width of the DUV pulse. At Kr pressures above 0.40 atm, $2\beta_{\text{pump}}$ was smaller than β_{idler}, so that the DUV pulse bandwidth increases monotonically with gas pressure. Based on these experimental results, we conclude that using a broader NIR spectrum does not necessarily produce a DUV pulse with a broader spectrum. The ratio of the frequency chirps of the idler and pump pulses, including those induced during FWM, need to be considered for broadband DUV pulse generation.

4 Conclusion

Satellite-free 10-fs DUV pulses were generated by BCP-FWM followed by dispersion compensation using prism and grating pairs. Positive GDDs induced in transparent media of up to 1000 fs^2 were compensated by the compressor in the laser system without inducing TOD. A nearly single pulse structure and smooth broad spectral profile were obtained for the DUV pulse. These features are useful when DUV pulses are applied to ultrafast spectroscopy. Narrowband DUV pulses were also obtained when the frequency chirps of the two input pulses cancelled out. Both the frequency chirps of the input pulses before the FWM interaction and the frequency chirp induced during nonlinear propagation inside the hollow fiber significantly influenced the DUV pulse bandwidth. The peak intensities (or pulse energies) of the input pulses, and thus the efficiencies of the SPM and cross-phase modulation induced inside the hollow fiber must be carefully considered when generating broadband DUV pulses or short DUV pulses by this approach.

Acknowledgements This work was supported by the Core Research for Evolutional Science and Technology (CREST) program of the Japan Science and Technology Agency (JST), National Science Council of the Republic of China, Taiwan (NSC 98-2112-M-009-001-MY3), and a grant from the Ministry of Education, Aiming for Top University (MOE ATU) Program at the National Chiao-Tung University (NCTU). A part of this work was performed under the joint research project of the Institute of Laser Engineering, Osaka University under Contract No. A3-01.

References

1. T. Kobayashi, Z. Wang, IEEE J. Quantum Electron. **44**, 1232 (2008)
2. T. Kobayashi, Z. Wang, New J. Phys. **10**, 065015 (2008)
3. T. Kobayashi, T. Saito, H. Ohtani, Nature **414**, 531 (2001)
4. I. Iwakura, A. Yabushita, T. Kobayashi, Chem. Lett. **38**, 1020 (2009)
5. I. Iwakura, A. Yabushita, T. Kobayashi, J. Am. Chem. Soc. **131**, 688 (2009)
6. C.G. Durfee, S. Backus, H.C. Kapteyn, M.M. Murnane, Opt. Lett. **24**, 697 (1999)
7. P. Baum, S. Lochbrunner, E. Riedle, Opt. Lett. **29**, 1686 (2004)
8. T. Fuji, T. Horio, T. Suzuki, Opt. Lett. **32**, 2481 (2007)
9. S.A. Trushin, K. Kosma, W. Fuß, W.E. Schmid, Opt. Lett. **32**, 2432 (2007)
10. F. Reiter, U. Graf, M. Schultze, W. Schweinberger, H. Schröder, N. Karpowicz, A.M. Azzeer, R. Kienberger, F. Krausz, E. Goulielmakis, Opt. Lett. **35**, 2248 (2010)
11. R.L. Fork, C.H. Brito Cruz, P.C. Becker, C.V. Shank, Opt. Lett. **12**, 483 (1987)
12. A. Shirakawa, I. Sakane, T. Kobayashi, Opt. Lett. **23**, 1292 (1998)
13. E. Zeek, K. Maginnis, S. Backus, U. Russek, M. Murnane, G. Mourou, H. Kapteyn, G. Vdovin, Opt. Lett. **24**, 493 (1999)
14. A. Baltuška, T. Fuji, T. Kobayashi, Opt. Lett. **27**, 306 (2002)
15. K. Okamura, T. Kobayashi, Opt. Lett. **36**, 226 (2011)
16. P. Tournois, Opt. Commun. **140**, 245 (1997)
17. N. Krebs, R.A. Probst, E. Riedle, Opt. Express **18**, 6164 (2010)
18. Y. Kida, J. Liu, T. Teramoto, T. Kobayashi, Opt. Lett. **35**, 1807 (2010)
19. S. Backus, J. Peatross, Z. Zeek, A. Rundquist, G. Taft, M.M. Murnane, H.C. Kapteyn, Opt. Lett. **21**, 665 (1996)
20. Y. Kida, T. Kobayashi, J. Opt. Soc. Am. B **28**, 139 (2011)
21. J.-C. Diels, W. Rudolph, *Ultrashort Laser Pulse Phenomena*, 2nd edn. (Academic Press, San Diego, 2006)